Investigation of exposure interval on the corrosion activities of Al 6061 hybrid nanocomposite in the acidic immersion corrosion experiment

S. Prathap Singh[1*], *J. Ajay*[1], *M. Akash*[1], *S. Arunkumar*[1], and *K. Yugandar*[1]

[1]Department of Mechanical Engineering, St. Joseph's Institute of Technology, Chennai, India

Abstract. This learning optimized corrosion determinant for Corrosion Rate (CR) of Aluminum (Al) 6061 base matrix alloy, strengthened by 0.6 wt.% Silicon Carbide (SiC) in addition with 0.2 wt.% Boron Carbide (B_4C) hybrid nano Metal Matrix Composite (MMC) manufactured using ultrasonic-aided stir casting. Nanoparticles raised the density of the Al 6061 alloy from 2.687 to 2.698 g/cm³. The Vicker's microhardness for hybrid nano MMC was 63.795 HV, which is 18% greater than the base raw Al 6061 alloy. The metallurgical investigation confirmed the presence and dispersion of green variety of SiC and higher hardness B_4C nanoparticles in the MMC, which produced intermetallic phases. Corrosion performance was evaluated in Sulphuric acid (H_2SO_4), Nitric acid (HNO_3) and Hydrochloric acid (HCl) acidic media at fluctuating dipping periods using a Taguchi L9 orthogonal array. Results showed that dipping durations and acid type significantly influenced the CR. The CR was uppermost in HCl and diminished with longer soaking due to passive layer formation.

1 Introduction

Material science advances have increased need for lightweight and durable operating resources in modern productions [1]. Nanoparticle-reinforced Al MMCs are stronger, stiffer, more wear-resistant, and better at high temperatures than unreinforced ones, hence modern materials science is interested in them [2,3]. Al-based nano MMC sites are used in defense, aerospace, nuclear, military, and automotive [4]. Creating an Al-based nano MMC is crucial, but standard stir casting struggles to distribute nanoparticles evenly throughout the alloy. This is caused by nanoparticles' high external area-to-volume fraction and poor wettability in molten metal [5].

Aykut Çanakçı *et al.* analyzed the wear and corrosion of AA2024/Hexagonal Boron Nitride (h-BN)/B_4C hybrid nano MMCs made using powder metallurgy. The hybrid nano MMC through 4 wt.% B_4C exhibits 14 intervals the wear opposition of unreinforced AA2024 matrix alloy. In corrosion testing, the hybrid nano MMC with 4 wt.% B_4C showed 47% higher corrosion resistance than the unreinforced AA2024 alloy [6]. Müslim Çelebi *et al.*

* Corresponding author : prathap.singh50@gmail.com

created hybrid Al Alloy-Alumina (Al_2O_3)-Graphite (Gr) nano MMC materials via powder metallurgy. Results show Al_2O_3 enhances mechanical properties. The hybrid nano MMC with 4 vol.% Al_2O_3 and 1vol.% Gr unveiled the utmost tensile power and hardness among others with different Al_2O_3 concentration [7]. Al nano MMC must have good grain shape, low porosity, and homogeneous nanoparticle distribution [8]. Ultrasonic-assisted stir casting is preferred because it consistently wets and disseminates nanoparticles in the alloy [9,10].

Corrosion behavior is a critical concern for Al6061 composites, especially in harsh environments. Studies using conventional homogeneous Al6061/SiC and B_4C composites have shown that SiC and B_4C content and test conditions significantly influence CRs. Sarapure *et al.* used the Taguchi design-of-experiments method to show that increasing SiC content (up to 4 wt.%) in Al6061 improved corrosion resistance in NaCl environments, with SiC wt.%, solution normality, and immersion duration identified as key factors [11]. Similarly, Uday *et al.* examined Al6061 and Al5052 strengthened with 5 - 10 wt.% SiC demonstrated that SiC content, solution concentration, and exposure time critically affected Sodium Chloride (NaCl) corrosion behavior [12].

Despite these advances, literature explicitly investigating the corrosion behavior of base Al 6061 grade matrix alloy, strengthened by 0.6 wt.% SiC in addition with 0.2 wt.% B_4C hybrid nano MMC remains sparse. Most prior work focuses either on mechanical and wear performance or on homogeneous systems. The corrosion influences local microstructure, including ceramic content, grain size, passive coating characteristics, and micro-galvanic interactions factors that determine the corrosion response. Yet, systematic studies that quantitatively correlate these spatial variations with CRs are missing.

This learning reports this understanding gap by analyzing the corrosion characteristics of base Al 6061 grade matrix alloy, strengthened by 0.6 wt.% SiC in addition with 0.2 wt.% B_4C hybrid nano MMC manufactured using ultrasonic-aided stir casting, precisely concentrating on the association among exposure duration and CR. Moreover, the effort includes microstructural categorisation, mechanical hardness plotting, and orderly designed corrosion analysis on the fabricated hybrid nano MMC.

2 Materials and Methods

2.1 Materials

Al 6061 alloy (2.7 g/cm³) was selected as the base matrix component for the fabrication of the Al 6061 - 0.6 wt.% SiC - 0.2 wt.% B_4C hybrid nano MMC due to its decent weldability, machinability, corrosion resistance, and workability. The alloy examined through the spectrometer confirmed the major component of Al with other alloying elements.

B_4C (2.52 g/cm³) and SiC (3.21 g/cm³) nanoparticles, with an average particle size of 60 nm, were nominated as the strengthening materials. B_4C is a multifaceted reinforcing agent compatible with various matrix constituents, owing to their comparable small density and remarkable abrasion resistance. Conversely, its extraordinary price has inadequate its extensive use. The majority of applications utilize SiC as a reinforcement since it is less expensive than B_4C. The Nano Research Lab, Jharkhand, India, provided the SiC and B_4C strengthening nanoparticles with the proper size and shape.

2.2 Manufacturing of hybrid nano MMC

Al 6061 - 0.6 wt.% SiC - 0.2 wt.% B_4C strengthened hybrid nano MMC was fabricated via an ultrasonic-aided stir casting approach. Initially, the furnace was set up at 700°C and left there for approximately 15 minutes to melt the necessary amount of Al 6061 alloy. Before progressively adding the B_4C and SiC nanoparticles to the molten material, the alloy mixture was mechanically agitated for 5 minutes at 600 rpm to make sure of uniformity, and the mechanical stirring process is publicized in Figure 1(a). After the addition of nano reinforcement elements, the ultrasonic probe was lowered into the molten mix at a penetration of 35 mm, and the ultrasonic wave originator was turned on for primary dispersion for 15 minutes. The ultrasonic processing was done for around 20 minutes. It generated a 20 kHz frequency for the ultrasonic cavitation effect using an ultrasonic generator with a Ti horn and the ultrasonic processing shown in Figure 1(b).

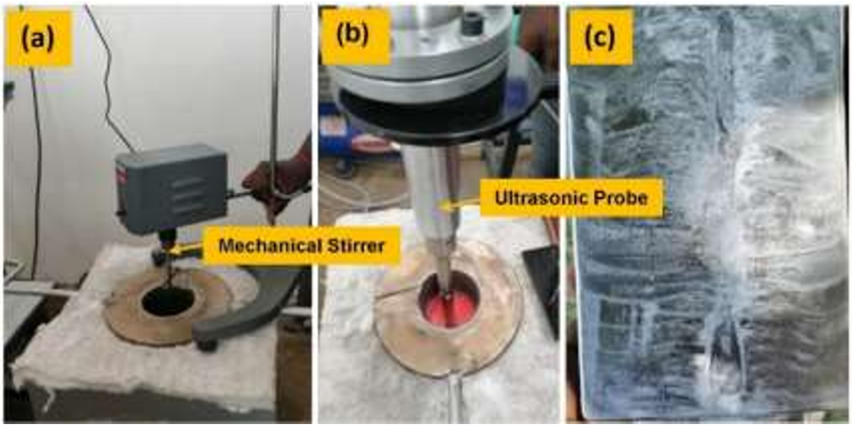

Fig. 1. (a) Mechanical stirring operation, (b) Ultrasonication operation, (c) Fabricated Al 6061 - 0.6 wt.% SiC - 0.2 wt.% B_4C hybrid nano MMC.

During processing, cavitation bubbles on the inside of the molten material form, and the liquid bindings are broken after the concentration of the ultrasonic waves is bigger than the energy of the melted Al adhesion energy. The random distribution of the surrounding particles in all directions is guaranteed by the collapse of the cavitation bubbles for the period of a high-pressure cycle. Consequently, effective ultrasonic processing greatly lowers the agglomeration tendencies of nanoparticles. Argon gas supplied during processing lessens the interaction among the molten material and the ambient gas. Because nanoparticles are added, the viscosity of the melt somewhat rises during sonication. So, to guarantee better melt flowability into the preheated (250°C) steel die, an upper casting temperature of 800°C was utilized following effective ultrasonic processing. Using the above method, Al 6061 alloy strengthened with B_4C and SiC hybrid nano MMC was synthesized with the wt.% of nano-sized SiC and B_4C being 0.6 and 0.2, respectively. The fabricated hybrid nano MMC with measurements of 150 x 100 x 10 mm in length, width, and thickness is shown in Figure 1(c).

2.3 Evaluation of physical, mechanical and metallurgical performances

The experiments in this study were conducted under controlled settings at 22°C and 50% relative humidity. These parameters fluctuated little, ensuring a consistent testing environment. The experimental density was evaluated on the base Al 6061 grade matrix alloy with the newly manufactured base Al 6061 grade matrix alloy - 0.6 wt.% SiC - 0.2 wt.% B_4C nano hybrid MMC through Archimedes methodology according to the ASTM D792 standard. The prepared and processed specimen was sliced with a measurement of 10 x 10 x 10 mm for density, hardness, and microstructure evaluation. The specimen's density was initially measured in air and subsequently in a liquid with a known density. The volume of liquid displaced by the specimen, when it is submerged, is equal to the density of the specimen.

The base Al 6061 grade matrix alloy with the manufactured base Al 6061 grade matrix alloy - 0.6 wt.% SiC - 0.2 wt.% B_4C nano hybrid MMC were examined for microhardness using Vicker's microhardness tester (Make: INNOVATEST, Model: Falcon 401) according to the ASTM-E384 standard. According to the specified standard, a 100 gf weight was made to indent on the hybrid nano MMC for a span of 15 seconds. Experiments were done at four specimen sites to rule out indenter-inflexible ceramic particle interaction. A mean of four dimensions was declared the Vicker's microhardness of the respective base matrix alloy and ceramic strengthened hybrid nano MMC.

The microstructure of the newly manufactured base Al 6061 grade alloy - 0.6 wt.% SiC - 0.2 wt.% B_4C nano hybrid MMC was comprehensively examined using an Olympus upright optical microscope. Thermo Fisher Scientific Inc.'s Version Apreo 2 was used for HRSEM and EDS to investigate material morphology. The cut specimen was prepared for metallurgical studies by polishing using different-grade grit papers. After polishing, the specimens were carved with Keller’s chemical component for 10 seconds.

2.4 Corrosion Testing

The primary acidic contact corrosion experiment was carried out to determine the CR of Al 6061 - 0.6 wt.% SiC - 0.2 wt.% B_4C hybrid nano MMC under the influence of weakened acids in the organic and acid management trades. The decomposition experimentation was carried out here by submerging specimens in 1M H_2SO_4, HNO_3, and HCl during a prolonged period of soaking.

The ceramic strengthened hybrid nano MMC samples were thoroughly washed using acetone and then weigh up using an accuracy weight apparatus with an accuracy of 0.001 grams and the experimentation was then commenced. The models were thereafter bringing out of the acidic immersion liquid at the restricted time and weigh up in order to determine the mass loss in order to determine the CR. Equation (1) delineates the formulation employed for the evaluation of the CR in mm/year.

$$CR = \frac{(K \times w)}{(A \times d \times t)} \tag{1}$$

Where K denotes the decomposition variable constant ($8.76*10^4$), w signifies the mass damage in grams, A represents the exterior area significantly affected by decomposition in cm^2, d indicates the density of the fabricated hybrid nano MMC experiment specimen in g/cm^3, and t reflects the period spent wrapped up in the various acidic liquid.

The experimentation design is supported by Taguchi L9 orthogonal array. The Taguchi method of carrying out design of experiments is simplest and clear. The method is effective to narrow down the research activity to few experiments. In this experiment, two corrosion determinant are considered, which are acidic solution and dipping time. Response is denoted by CR.

Table 1. Stages of contribution corrosion determinant.

Levels	Acidic liquid medium	Exposure interval (Hours)
1	HCl	48
2	H_2SO_4	144
3	HNO_3	216

In the Taguchi approach, two important factors are used to determine the appropriate orthogonal array; These are: This paper outlines the significant input and response components, and the seminal relations. Input variables have two levels of evidence. Predicted results of experimentation, cost and efficacy constraints. As it is reported in the existing works, Table 1 shows the three corrosion determinant, which are divided into three dissimilar stages. The experimentation design matrix is developed through Taguchi approach in MINITAB 21 software; Table 2 illustrates it.

Table 2. Design matrix and examined consequences.

Run No	Acidic liquid medium	Exposure duration (Hours)	CR (mm/year)
1	HCl	48	22.31
2	HCl	144	10.65
3	HCl	216	5.81
4	H_2SO_4	48	14.34
5	H_2SO_4	144	7.8
6	H_2SO_4	216	6
7	HNO_3	48	8.08
8	HNO_3	144	4.39
9	HNO_3	216	1.83

3 Results and Discussions

3.1 Physical and Mechanical Evaluation

The density of the obtained base Al 6061 grade matrix alloy and the performance enhanced Al 6061 grade matrix alloy by the inclusion of 0.6 wt.% SiC in addition with 0.2 wt.% B_4C nano hybrid MMC are 2.687 and 2.698 g/cm^3 respectively. The hybrid nano MMC outweighed the Al6061 alloy as measured by density. This could potentially be attributed to the high-density nano reinforcements of SiC and B_4C.

The hybrid nano MMC (63.795 HV) exhibited an increase in Vicker's microhardness, surpassing the base Al 6061 matrix alloy (54.03 HV) by 18%. This phenomenon may be owing to the significant exterior surface zone enhancement provided by the SiC and B_4C hard ceramic strengthening nanoparticles within the base Al matrix 6061 grade alloy. The enhanced microhardness characteristics of the nano hybrid MMC can be recognised primarily to the dissemination of hard ceramic strengthening nanoparticles. Perumal *et al.* observed a comparable rise in Vicker's microhardness after the inclusion of different nano strengthening hard ceramics such as SiC, Al_2O_3, and titanium dioxide [13].

3.2 Metallurgical Evaluation

Figures 2(a) and (b) show the optical microstructure of the 0.6 wt.% SiC in addition with 0.2 wt.% hard ceramic B_4C hybrid nanoelements reinforced with Al 6061 MMC at 100X and 500X magnification, respectively. It showed the existence of α Al regions and the primary eutectic Silicon (Si) regions with nano reinforcements such as SiC and B_4C particles.

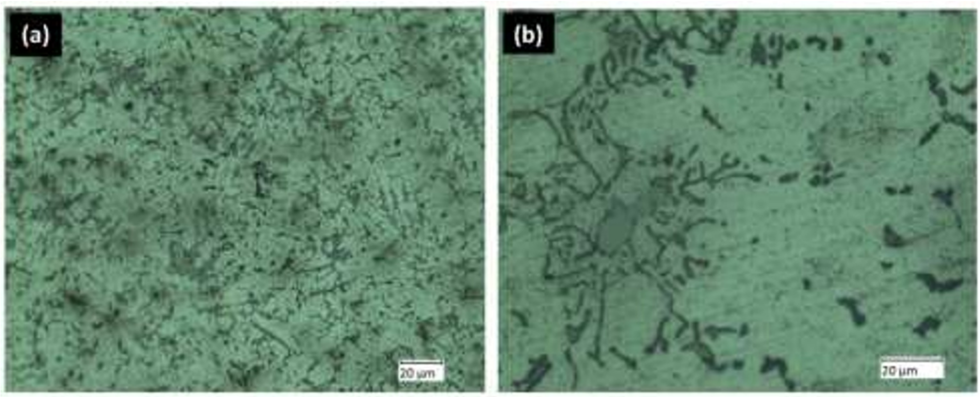

Fig. 2. Microstructure of Al 6061 hybrid nano MMC at (a) 100X; (b) 500X.

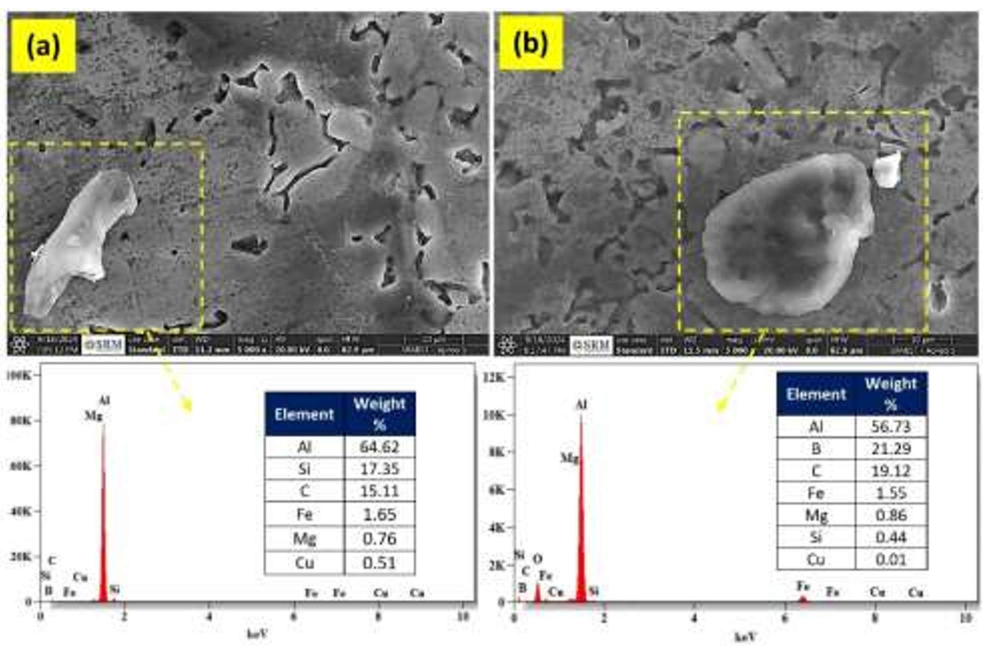

Fig. 3. HRSEM appearance of Al 6061 grade alloy hybrid nano MMC with (a) SiC nanoparticles with corresponding EDS, (b) B_4C nanoparticles with corresponding EDS.

Figures 3(a) and 7(b) showed the HRSEM of identified hard ceramic SiC and B_4C reinforcement particles in the both nanoparticles reinforced with Al 6061 MMC along with its EDS analysis. The reinforcement particles were confirmed through the existence of Si, B, and C. The remaining particles, such as Fe, Mg, and Cu, confirmed the elements of the base Al 6061 matrix alloy. Figure 3(a) showed SiC nanoparticles and confirmed that there were more Si and carbon in the EDS analysis. On the other hand, Figure 3(b) demonstrated the presence of B_4C nanoparticles, confirming a higher wt.% of boron and carbon elements in the EDS analysis. Prashant and Thomas found similar nano particle dispersion in their Al 7075 alloy, which was strengthened with SiC, Gr, and Al_2O_3 nano particles [9].

3.3 Statistical exploration of CR

The Minitab software generated the response table for SNR from the comparable CR values. Table 3 shows the order of control of corrosion determinants such as acidic liquid medium and exposure length on the primary response such as CR. The examined delta value measured the control of the corrosion determinant. The delta value was calculated by subtracting the supreme and least SNRs of the corrosion determinant. The perception of acidic liquid medium had the greatest effect on the CR, followed by the duration of exposure.

Table 3. Response Tabulation for SNRs of the CR.

Level	Acidic liquid medium	Exposure duration
1	-18.85	-22.75
2	-20.93	-17.08
3	-12.08	-12.03
Delta	8.85	10.72
Rank	2	1

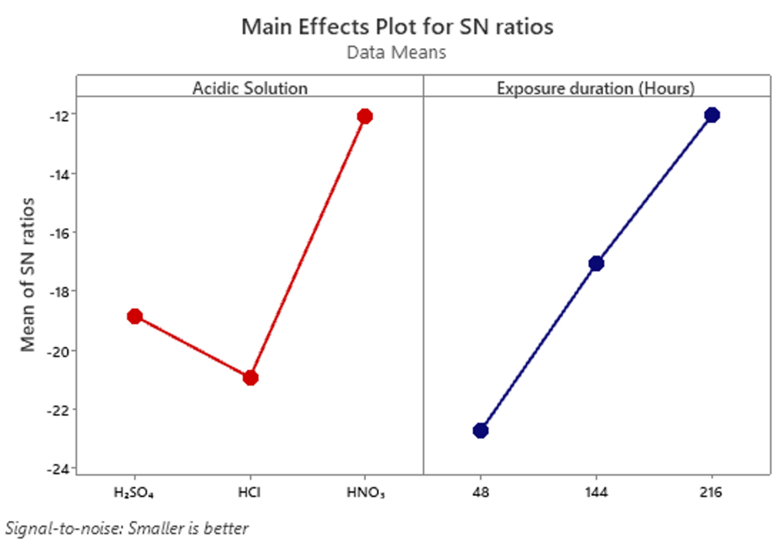

Fig. 4. SNR response plot for the CR to reading the significant impression of corrosion determinants.

Figure 4 displays the diagrams shown for CR and SNRs, with the supreme SNRs for each and respective corrosion determinant providing the optimal set of values for corrosion determinants. A 216-hour exposure to an acidic HNO_3 solution yielded the best corrosion determinants for achieving a minimal CR.

Analysis of Variance (ANOVA) was used to determine the significance proportion stage of the corrosion determinants, as shown in Table 4. The exploration was conducted with a confidence level of 95 percent. The level of relevance of CR was highest for exposure length

(56.21%), followed by acidic solution (33.17%). For longer exposure times, the corrosion determinant makes a significant contribution to the SR.

Table 4. ANOVA consequence for the evaluated CR.

Source	DF	Adj SS	Adj MS	F-Value	P-Value	Percentage of contribution (%)
Acidic liquid medium	2	100.37	50.185	6.25	0.059	33.17
Exposure duration	2	170.04	85.022	10.59	0.025	56.21
Error	4	32.10	8.025			10.62
Total	8	302.51				

3.4 Influence of corrosion determinant on the CR

Figure 5 shows how corrosion determinants affect CR in the Al 6061 - 0.6 wt.% SiC - 0.2 wt.% B_4C hybrid nano MMC. Figure 5 shows that hybrid nano MMC samples in HCl acidic medium had a supreme CR of 22.31mm/year, higher than those in H_2SO_4 and HNO_3. The hybrid nano MMC sample dipped in HCl acidic combination had the greatest effect, presumably due to its intense reactivity and forceful surface attack. Prathap *et al.* obtained a similar maximum CR for the Al 6061 alloy when it was immersed in an HCl solution [14]. On the other hand, sulphuric and nitric acidic liquid medium may form passive coatings or a smaller amount aggressive interfaces. Immersion of hybrid nano MMCs in HCl acidic medium with chloride ions increases corrosion. Water ionization creates chloride ions from HCl. Chloride ions damage the hybrid nano MMC 's stiff aluminium oxide passive metal layer. After removing the tough oxide liner, chloride ions enter the hybrid nano MMC through circumferential micro-cracks, eliminating hydrogen bubbles to create aluminium chloride. The pitting CR development begins.

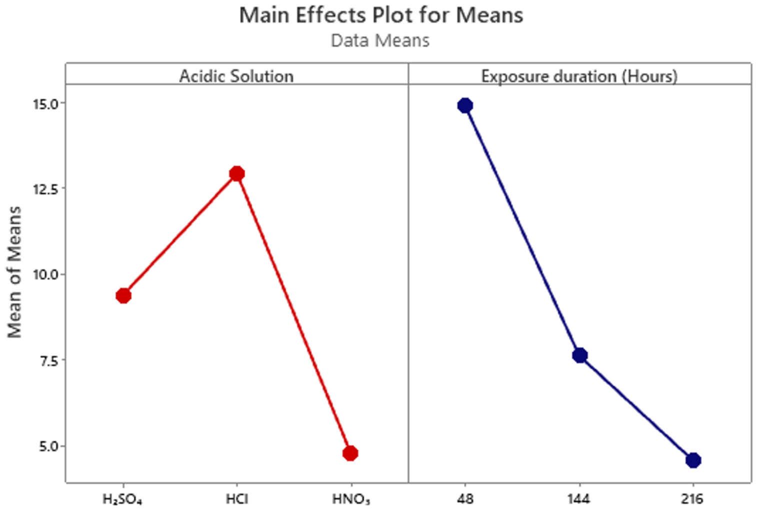

Fig. 5. Inspiration of corrosion determinants on the response of CR.

Increasing dipping duration decreased hybrid nano MMC CR. The CR crests at 48 hours and drops sharply at 144 and 216 hours. Hybrid nano MMC corrosion resistance rises 48 hours after chloride ion absorption. For 144 - 216 hours, corrosion declines steadily. A unchanging passive coating of aluminium hydroxide grows on composite surfaces regardless of reinforcement. Maximum corrosion may occur at this time due to the passive layer. This passive layer prevents corrosion.

3.5 Worn exterior surface characterization

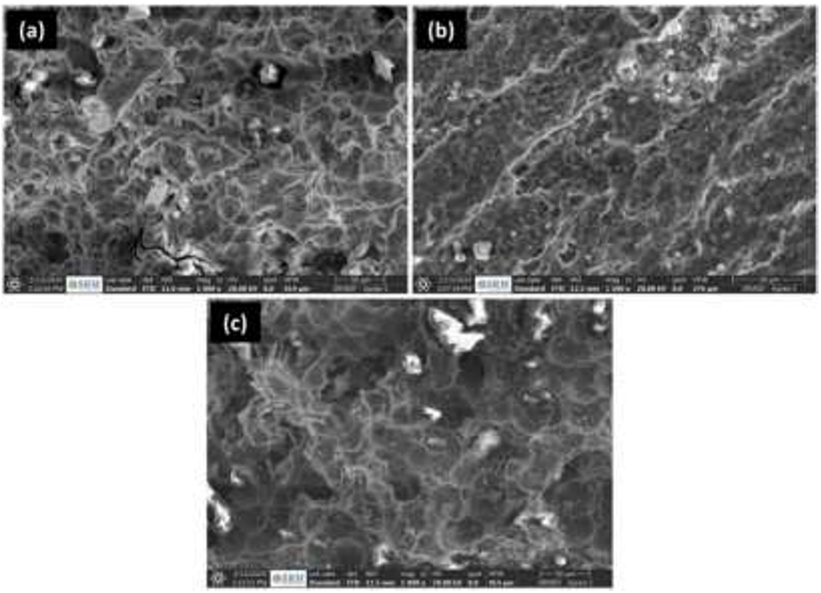

Fig. 6. HRSEM appearance of the hybrid nano MMC corroded model exterior in (a)HCl, (b) H_2SO_4, (c) HNO_3

Figure 6(a-c) depicts the instrument captured HRSEM picture of the Al 6061 - 0.6 wt.% SiC - 0.2 wt.% B_4C hybrid nano MMC damaged sample after immersion in several acidic solutions. Figure 6(a) shows an instrument captured HRSEM picture of a hybrid Al 6061 grade nano MMC sample immersed in HCl acidic liquid medium, revealing damages due to specific location corrosion with preferential base Al 6061 grade matrix attack surrounding hard strengthening ceramic such as SiC and B_4C nanoparticles owing to micro-galvanic properties in a hydrochloric acidic environment. Figure 6(b) displays an instrument captured HRSEM picture of a hybrid Al 6061 grade nano MMC immersed in H_2SO_4 acidic liquid medium, revealing negligible exterior area damage owing to restricted corrosive contact. Figure 6(c) demonstrates the instrument captured HRSEM picture of the hybrid Al 6061 grade nano MMC dipped in HNO_3 acidic liquid medium, which exhibited a small attack on the external surface due to minimal surface damages.

4 Conclusion

In this study, the Al 6061 strengthened with the inclusion of 0.6 wt.% SiC in addition with 0.2 wt.% B_4C nano hybrid MMC was fabricated and corrosion behaviour was optimized to control the corrosion determinant. The following decisions were attained from this experimental investigation:

The density analysis indicated an elevated density of 2.698 g/cm³ in the hybrid nano MMC, attributed to the incorporation of hard strengthening nano SiC and B_4C strengthening nanoparticles. Moreover, the evaluation of Vicker's microhardness revealed an increase in microhardness, measuring 18% greater than that of the Al 6061 alloy. This phenomenon can be recognized to the presence and even dissemination of nano elements within the hybrid nano MMC.

The optical microstructure and HRSEM scrutiny established the existence of α Al with nano-sized SiC and B_4C particles. The EDS and elemental mapping evaluation confirmed the Al alloy and nanoparticles presence through the attendance of individual periodic table particles such as Al, C, Fe, Si, B, Mg, and Cu.

Acidic solution and dipping duration both had a substantial effect on CR. HCl generated the furthermost dangerous corrosion, while HNO_3 had the slightest attack owing to passive coating development.

References

1. P. Verma, J. Ghose, G. Paul, V. Pandey, U. Pandey, Enhanced mechanical and tribological performance of AA2014-SiC metal matrix nanocomposites fabricated by a novel stir-ultrasonic-squeeze casting process. Int. J. Cast Met. **38(1)**, 21-35 (2025). https://doi.org/10.1080/13640461.2025.2469026
2. M. Ekpu, Sunday C. Ikpeseni, Characterising the Mechanical Properties of a Composite Material Comprising Aluminium and Silicon Carbide. Silicon. **16**, 4333-4342 (2024). https://doi.org/10.1007/s12633-024-03006-8
3. D. Periyasamy, J. Duraisamy, Sami Al Obaid, V. Rathinavelu, Aluminium Alloy Nanocomposite Featured with Barium and Silicon Carbide Nanoparticles: Mechanical and Wear Studies. Silicon. **17**, 1165-1176 (2025). https://doi.org/10.1007/s12633-025-03263-1
4. Huijie Zhang, Baoxin Zhang, Qiuzhi Gao, Jianling Song, Guoliang Han. A review on microstructures and properties of graphene-reinforced aluminum matrix composites fabricated by friction stir processing. J. Manuf. Process. **68(B)**, 126-135 (2021). https://doi.org/10.1016/j.jmapro.2021.07.023
5. L. Osunmakinde, T. B. Asafa, P. O. Agboola, M. O. Durowoju, A Systemic review of the influence of eco-friendly particles on hybrid composites synthesized via stir casting technique. Discov Mechanical Engineering **3**, 32 (2024). https://doi.org/10.1007/s44245-024-00055-6
6. Aykut Çanakçı, Abdullah Hasan Karabacak, Müslim Çelebi, Serdar Özkaya, Kür¸sat Alp Arpacı. A Study on the Optimization of Nano-B_4C Content for the Best Wear and Corrosion Properties of the Al-Based Hybrid Nanocomposites. Arab J Sci Eng **49**, 14625–14641 (2024). https://doi.org/10.1007/s13369-024-08736-w
7. Müslim Çelebi, Onur Güler, Aykut Çanakçı, Hamdullah Çuvalcı. The effect of nanoparticle content on the microstructure and mechanical properties of ZA27-Al_2O_3-Gr hybrid nanocomposites produced by powder metallurgy. Journal of Composite Materials. **55(24)**, 3395-3408 (2021). https://doi.org/10.1177/00219983211015719
8. G. Rajan, A. Kumar, S. Mula, Influence of friction stir processing on wear behavior of nanosized SiC reinforced AA5083 nanocomposites developed by stir casting. J. Manuf. Process. 141, 1631-1649 (2025). https://doi.org/10.1016/j.jmapro.2025.03.065
9. P.S. Tile, B. Thomas. Effect of Load, Sliding Velocity, and Reinforcements on Wear Characteristics of Al7075-Based Composite and Nanocomposites Fabricated by Ultrasonic-Assisted Stir-Casting Technique. Inter Metal cast **18**, 180-195 (2024). https://doi.org/10.1007/s40962-023-01006-9

10. P.K. Dinesh Kumar, S. Darius Gnanaraj. Characterization of Al-Si Alloy Reinforced with B_4C and TiO_2 Nanoparticles. Silicon **16**, 4437-4449 (2024). https://doi.org/10.1007/s12633-024-03012-w
11. Sadanand Sarapure, B. P. Shivakumar, M. B. Hanamantraygouda, Investigation of Corrosion Behavior of SiC-Reinforced Al 6061/SiC Metal Matrix Composites Using Taguchi Technique. J Bio Tribo Corros. **6**, 31 (2020). https://doi.org/10.1007/s40735-020-0328-3
12. K. N. Uday, K. Senthilraj, Rajamurugan Govindasamy, Prabu Krishnasamy, Study of NaCl Corrosion Behavior on SiC-Reinforced in Al 6061 and Al 5052 Metal Matrix Composites Using Taguchi's Technique, SAE Technical Paper (2022). https://doi.org/10.4271/2022-28-0531
13. G. Perumal, N. Senthilkumar, Nithesh Naik, B. Deepanraj, Comparative assessment of the mechanical, tribological, and corrosion properties of Al/SiC/Al_2O_3 and Al/SiC/TiO_2 hybrid composites. Discov Appl Sci. **7**, 237 (2025). https://doi.org/10.1007/s42452-025-06687-x
14. S. Prathap Singh, M. Gerald Arul Selvan, P. Jose Aloysius, P. Ravichandran, K. Vinoth Babu, Effect of acidic solution and immersion duration on the corrosion behaviour of the aluminium 6061 alloy, Mater. Today Proc. (2023). https://doi.org/10.1016/j.matpr.2023.08.232